

Wide-band, high-resolution soft x-ray spectrometer for the Electron Beam Ion Trap

G. V. Brown, P. Beiersdorfer, and K. Widmann

Lawrence Livermore National Laboratory, 7000 East Avenue, Livermore, California 94550

(Presented 8 June 1998)

We have constructed two wide-band, high-resolution vacuum flat crystal spectrometers and implemented them on the Electron Beam Ion Trap located at the Lawrence Livermore National Laboratory. Working in unison, these spectrometers can measure an x-ray bandwidth ≤ 9 Å in the soft x-ray region below 21 Å. In order to achieve this large bandwidth each spectrometer houses either two 125 mm \times 13 mm \times 2 mm RAP (rubidium acid phthalate, $2d=26.121$ Å), two 114 mm \times 13 mm \times 2 mm TIAP (thallium acid phthalate, $2d=25.75$ Å) crystals, or some combination thereof, for dispersion and two position sensitive proportional counters for detection of x rays. The spectrometers are used to measure wavelengths and relative intensities of the *L*-shell line emission from Fe XVII–XXIV for comparison with spectra obtained from astrophysical and laboratory plasmas. The wide wavelength coverage attainable by these spectrometers makes it possible to measure all the *L*-shell emission from a given iron ion species simultaneously. © 1999 American Institute of Physics. [S0034-6748(99)59801-8]

I. INTRODUCTION

X-ray spectroscopy has provided valuable data from a number of astrophysical sources such as stellar coronae,¹ supernova remnants,² and solar active regions.^{3–8} Beginning with the discovery of x rays in the Sun in 1948,⁹ the wealth of information derived from x-ray emission from astrophysical sources has driven the development of highly sophisticated satellite missions designed for spectroscopic measurements such as *Solar Maximum Mission* (SMM) and the *Advanced Satellite for Cosmology and Astrophysics* (ASCA) and to upcoming x-ray satellite missions such as the *Advanced X-ray Astrophysics Facility* (AXAF) and the *X-Ray Multi-Mirror Mission* (XMM) which boast higher resolution and throughput than their predecessors.

X-ray spectroscopy has also been used extensively in the study of high-temperature laboratory plasmas. A measurement of iron *L*-shell emission from the PLT tokamak, for example, shows a plethora of lines in the 6–17 Å region from many charge states.¹⁰ Interpreting the data from laboratory, solar, and astrophysical plasmas requires a thorough understanding of the underlying atomic data. Because of its complexity, the physical understanding of the *L*-shell iron spectrum in the ultrasoft x-ray region is still incomplete. For example, spectral fitting of the iron *L*-shell emission obtained with the ASCA satellite has revealed a deficit in the 8–10 Å range.^{11–13} This deficit could be understood by recent measurements at our EBIT facility that showed that there is a significant amount of radiative flux in the *L*-shell transitions that emanate from levels with high principal quantum number *n*.¹⁴ For example, the amount of flux in the transitions $nd \rightarrow 2p$ in Fe XVII with $n \geq 5$ and all $np \rightarrow 2s$ with $n=4$ and 5 is 13% of the amount of the $3d \rightarrow 2p$ resonance line. Because these lines are comparatively weak and typically blend with lines from higher charge states, they had not been observed in previous laboratory measurements and

had not been included in spectral modeling codes. Additional laboratory measurements under well controlled conditions are clearly needed to develop the iron *L*-shell emission in the 6–17 Å region into a reliable spectral diagnostic of high-temperature plasmas.

In order to measure wavelengths, relative line strengths, and excitation cross sections with high accuracy in the soft x-ray regime (≤ 25 Å) for use in data bases employed by the spectral fitting packages, we have designed, built, and implemented a pair of nearly identical vacuum crystal spectrometers for use at the Electron Beam Ion Trap (EBIT) Facility located at the Lawrence Livermore National Laboratory. The Electron Beam Ion Trap was designed for spectroscopy of highly charged ions under precisely controlled conditions and has been used extensively for x-ray measurements.^{15,16} The two spectrometers, one designated the “Orange” and the other the “Blue” broad-band spectrometer, have a design that extends the design of high-resolution flat crystal spectrometers employed previously on EBIT.^{17,18}

The spectrometers diffract x rays according to Bragg’s law of crystal diffraction given by

$$n\lambda = 2d \sin(\theta), \quad (1)$$

where *d* is the lattice spacing of the crystal and θ is the incident angle. Operating in the range of Bragg angles $0^\circ \leq \theta \leq 58^\circ$, the Orange and Blue broadband spectrometers work in unison to cover an x-ray bandwidth of ~ 9 Å. Because the largest x-ray bandwidth of *L*-shell emission of an ion of iron is less than 8 Å, these spectrometers make possible the simultaneous measurement of the complete *L*-shell emission from one ionic species of iron. It is therefore possible to make accurate determinations of the wavelengths, relative line intensities, and excitation cross sections for one ionic species of iron without realigning the spectrometer in a single measurement. This contrasts strongly with the need

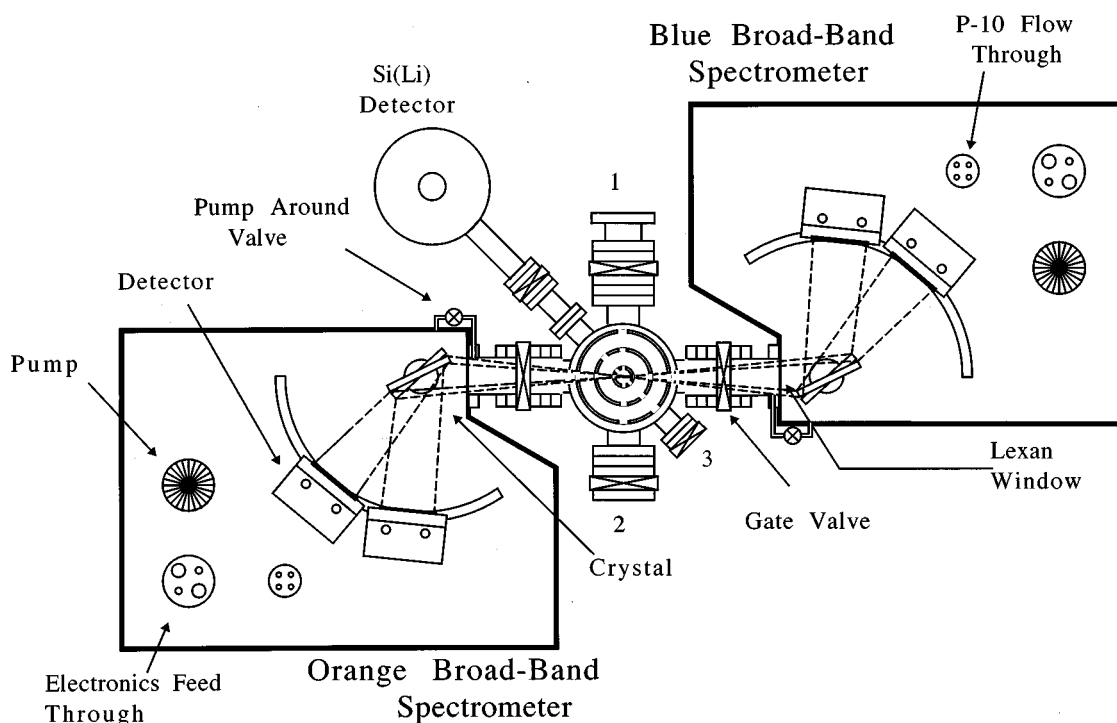


FIG. 1. Top view of the Orange and Blue spectrometers on EBIT. Each spectrometer houses two crystals and two detectors. The electron beam is perpendicular to the page. Ports labeled 1, 2, and 3 are generally equipped with a flat field spectrometer, a von Hámos curved crystal spectrometer, and a gas injector, respectively.

for nine overlapping spectral measurements to cover the 10–17 Å region in previous studies on EBIT¹⁴; as a consequence of the 1.5 Å bandwidth of the spectrometers previously employed on EBIT.

II. SPECTROMETER DESIGN AND IMPLEMENTATION

The Orange and Blue wideband, high-resolution spectrometers are connected to EBIT via gate valves 180° apart, i.e., on opposite x-ray ports, and are oriented at an angle of 90° to the beam (Fig. 1). In order to avoid the absorption of soft x-rays by air, each spectrometer operates at a pressure of $\sim 10^{-5}$ Torr. To prevent the vacuum of the spectrometers from compromising the vacuum of EBIT ($\sim 10^{-10}$ Torr) when the spectrometer is acquiring data (gate valve open), each spectrometer is separated from the chamber of EBIT by a freestanding 2.5"×1" lexan window either 0.5 or 1.0 μm thick. The size of the window is chosen so that the spectrometer is able to view the entire 8° of opening angle allowable by EBIT's x-ray ports. This is twice the angle accessible with the previous flat crystal spectrometers.^{17,18} To prevent the window from rupturing when the gate valve is closed, each spectrometer has been equipped with a "pump around" valve (Fig. 1) which, when open, connects the vacuum chamber of the spectrometer to the small volume between the lexan window and the gate valve providing equal pressure to both sides of the lexan window. This design has been implemented on both previous generation vacuum flat crystal spectrometers employed on EBIT.^{17,18}

Each of the spectrometers houses either two 125 mm × 13 mm × 2 mm RAP (rubidium acid phthalate, $2d = 26.121$ Å¹⁹) two 114 mm × 13 mm × 2 mm TIAP (thallium acid phthalate, $2d = 25.75$ Å¹⁹) crystals, or some com-

bination thereof, for diffraction of x rays. These crystals are twice as long but only half the height of those used previously.^{17,18} In order to mount the crystals in the spectrometers, each crystal is attached to a 114 mm or 125 mm × 13 mm × 13 mm aluminum substrate. The substrates are mounted in the spectrometer such that the axis of rotation of each crystal is 38 cm from the electron beam and with one crystal positioned slightly below the center of the x-ray port and one slightly above the center of the x-ray port. This arrangement allows use of a single EBIT port for two spectrometer arms and sightlines concurrently. The lower crystal substrate is mounted directly to a rotatable stage, and the upper crystal substrate is suspended from a support structure which is attached to a separate rotatable stage. The upper crystal's support structure produces a constraint on the maximum angle between the two crystals of 55° because at this angle the support structure comes into contact with the substrate of the lower crystal. Each stage is attached to a mechanical vacuum feed through making it possible to rotate each crystal independently from outside the spectrometer housing. It should be noted that these spectrometers have been designed to accommodate crystals which are 114 mm long, hence crystals which are less than 114 mm in length can be rotated from 0° to beyond 90°. However, when using crystals which are greater than 114 mm long, there are limits to the maximum and minimum achievable Bragg angle. For example, when using the 125 mm long RAP crystal, the substrate comes into contact with the wall of the spectrometer housing at an angle of $\sim 70^\circ$ and the crystal comes into contact with the lexan window at an angle of $\sim 16^\circ$.

In order to detect the diffracted x rays, the orange and blue spectrometers each employ two single wire position

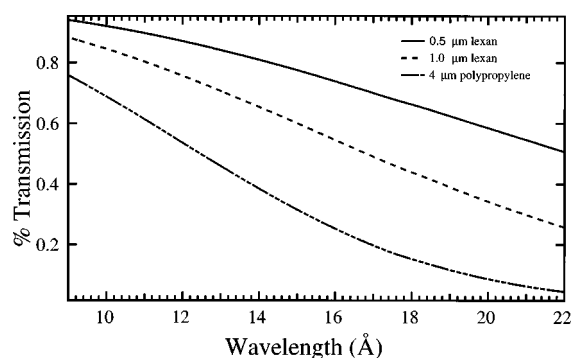


FIG. 2. Transmission curves for foils between EBIT and the detector.

sensitive proportional counters, i.e., one detector for each crystal. The detectors use the resistance-capacitance position encoding method for determining the position of the incident photon²⁰ with a spatial resolution of $\sim 250 \mu\text{m}$ at the x-ray energies of interest. The detector's fill gas is P-10 (90% argon and 10% methane), which flows through the detector at a rate of about $1 \text{ mm}^3/\text{s}$. The pressure in the detector is 1 atm. The detector window is made of $4 \mu\text{m}$ polypropylene coated with $200\text{--}400 \text{ \AA}$ of aluminum with an active area of $10 \times 0.8 \text{ cm}^2$. The center of the detectors are 25.4 cm from the crystal's axis of rotation with each detector being slightly offset either below or above the center of their respective source crystals so as to maximize the detected flux from EBIT. This is based on the assumption that the flux from the trap is a maximum at its center. The detectors are attached to mechanical arms which move each detector along a common rail from outside of the spectrometer using a mechanism similar to that used to rotate the crystals. Hence, the detectors can also be positioned from outside the spectrometer while preserving its vacuum. Because both detectors move along a common rail, there is a minimum angle between the centers of each detector of $\sim 30^\circ$, which occurs when their housings come into contact with one another. The walls of the spectrometer and its orientation on EBIT limit the maximum angle of one detector to $\sim 110^\circ$. This makes the maximum angle achievable by the second detector $\sim 80^\circ$.

The polypropylene window used on the detectors and the lexan window used to separate the spectrometer vacuum chamber from EBIT's vacuum chamber have energy dependent responses where, in general, photons with higher energy are transmitted more efficiently than those with lower energy. The response curve for each foil has been calculated and can be accounted for in our measurements. The transmission of the lexan $0.5 \mu\text{m}$ foil varies from above 90% for energies above 1200 eV down to 65% for energies around 700 eV .²¹ The polypropylene foils have higher absorption coefficients and transmit below 15% at energies below 700 eV .²¹ This increases to a transmission of about 60% at 1200 eV . Figure 2 shows the calculated response curves as a function of wavelength for the 0.5 and $1.0 \mu\text{m}$ lexan and the $4 \mu\text{m}$ polypropylene windows. Transmission of the various foils had been measured in earlier investigations²² and found good agreement with these calculations.

The constraints on the relative positions of the two detectors and the two crystals, the maximum and minimum

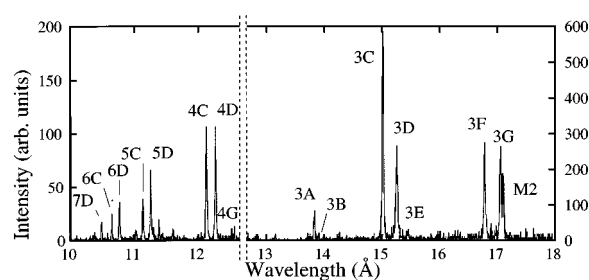


FIG. 3. Spectrum of L -shell emission of Fe XVII observed by three of the four spectrometer arms. The connections are made at 15.16 and 12.20 \AA . The lines have been previously identified by Brown *et al.* (1998) and are labeled in the scheme of Parkinson (1972). It should be noted that the scale for the region below 12.7 \AA is a factor of 3 less than that for the region above 12.7 \AA .

allowable angles, the dimensions of the crystals and detector windows along with the dimensions of the spectrometer housing provide a measurable Bragg angle range from 0° to 58° . The limiting factor of the largest Bragg angle is the maximum angle of 110° achievable by the center of the detector. The constraints on the crystal and detector positions, and the fact that even when the crystal is able to subtend the entire opening angle of 8° the maximum spectral coverage of one RAP crystal is 3.5 \AA at a Bragg angle of 16° , make it necessary to use both the orange and blue spectrometers in unison to achieve a spectral range of 9 \AA (7.5 \AA continuous) from 9 to 18 \AA .

III. MEASUREMENT

Here, we present a measurement by the orange and blue spectrometers of all line emission from the L shell of Fe XVII which falls in the wavelength band between 9.8 and 17.1 \AA (see Fig. 3). The spectrum was acquired at an electron beam energy of $1200 \pm 30 \text{ eV}$, a beam current of 25 mA , and an electron density of $0.5\text{--}1 \times 10^{12} \text{ cm}^{-3}$. It is labeled in the notation of Parkinson.²³ The crystals used are three $125 \text{ mm} \times 13 \text{ mm} \times 2 \text{ mm}$ RAP crystals. The resolving power demonstrated by this measurement is $\lambda/\Delta\lambda = 500\text{--}700$. Whereas previous measurements of this same spectrum required nine different spectrometer settings,¹⁴ the present measurement only required one, thus reducing the acquisition time by nearly an order of magnitude. An example of the bandwidth of a single crystal in the Blue spectrometer is given in Fig. 4. This shows a wavelength spread of nearly 3 \AA .

To span the wavelength range from $9.8\text{--}17.1 \text{ \AA}$ requires both RAP crystals in the Orange spectrometer and one in the Blue spectrometer. The crystals are set to Bragg angles such that the Orange spectrometer spans the regions between $9.7\text{--}12.2$ and $15.0\text{--}17.1 \text{ \AA}$ and the Blue spectrometer spans the region between 12.1 and 15.1 \AA . Note that the ranges are chosen to overlap. The overlapping regions between adjacent spectra are used for normalization. Each of the overlapping regions contain a strong Fe XVII line. In the region of overlap between the lowest wavelength region and the middle region the line $4D$ is used for cross normalization, and in the region between the middle and the upper wavelength region the line $3C$ is used. Figure 4 shows the spectrum that bridges the

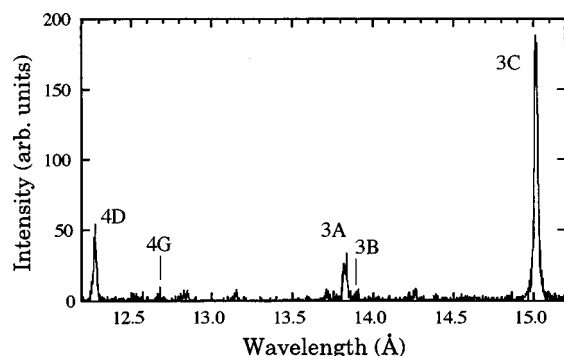


FIG. 4. Spectrum with a single spectrometer arm. The spectrum covers 2.9 Å and demonstrates that nearly the full 8° of opening angle is subtended by the crystal.

long- and the short-wavelength spectra. Here, line 3C is at the long-wavelength side, 4D is at the short-wavelength side.

Each of the three spectra are corrected for the response of both the lexan and polypropylene windows. Because the Blue spectrometer has a 1 μm thick lexan window while the window on the Orange is 0.5 μm thick, the window response function for each spectrometer are not equal. After removing the response of the foils from each of the spectra, the lines that are common to adjacent spectra should have an equal number of counts; however, this is not the case. Line 4D in the lower spectrum is greater than that in the middle spectrum by 25%, and 3C is 20% greater in the middle spectrum than in the upper spectrum. The true source of this difference is not known, although it is believed to be related to the alignment of the spectrometers relative to the trap region. In order to account for these differences when concatenating adjacent spectra, the spectra were each scaled so that the areas in the common lines were equal. It should be noted that since the source is based on a unidirectional electron beam it produces polarized radiation,^{24,25} and the crystals act as polarizers²⁶ it is necessary to account for this effect when determining accurate line intensities; however, for the measurement presented here no adjustment for the crystal response nor polarization effects has been made. The average value between the Mosaic and the Darwin-Prins integrated reflectivity calculated by Henke *et al.*²⁷ decreases by 30% from 9.7 to 17.3 Å for nonpolarized line emission. The sensitivity variations presented here based on the spectrum corrected for transmission of the foils and the normalization between three spectra with no correction for crystal response is believed to be reliable to within 12%–15% over the entire wavelength range observed.

Although not presented here, these spectrometers have made possible the measurement of all the significant resonant, dielectronic, and direct excitation cross sections for the *L*-shell emission of Fe XVII as a function of energy, conducted during a two-week (300 h) measurement period. Such an endeavor would have been impossible without the large bandwidth of these spectrometers that reduced acquisition time by about an order of magnitude.

ACKNOWLEDGMENTS

The authors would like to thank K. Visbeck, E. Magee, and D. Nelson for their technical support. This work was performed by the Lawrence Livermore National Laboratory under the auspices of the U.S. D.O.E. under Contract No. W-7405-ENG-48 and supported by NASA under work order No. W-19127.

- ¹P. W. Vedder and C. R. Canizares, *Astrophys. J.* **270**, 666 (1983).
- ²P. F. Winkler *et al.*, *Astrophys. J.* **246**, 27 (1981).
- ³R. L. Blake, T. A. Chubb, H. Friedman, and A. E. Unizicker, *Astrophys. J.* **142**, 1 (1965).
- ⁴F. F. Freeman and B. B. Jones, *Sol. Phys.* **15**, 288 (1970).
- ⁵J. H. Parkinson, *Sol. Phys.* **42**, 183 (1975).
- ⁶R. H. Hutcheon, F. P. Pye, and K. D. Evans, *Mon. Not. R. Astron. Soc.* **175**, 489 (1976).
- ⁷D. L. McKenzie *et al.*, *Astrophys. J.* **241**, 409 (1980).
- ⁸K. J. H. Phillips *et al.*, *Astrophys. J.* **256**, 774 (1982).
- ⁹J. D. Purcell, R. Tousey, and K. Watanabe, *Phys. Rev.* **76**, 165 (1949).
- ¹⁰S. von Goeler *et al.*, in *Diagnostics for Fusion Reactor Conditions*, edited by P. S. *et al.* (Commission of the European Communities, Belgium, 1982), p. 109.
- ¹¹N. E. White, in *Cool Stars, Stellar Systems, and the Sun*, edited by R. Pallavicini and A. K. Dupree (Astronomical Society of the Pacific, San Francisco, CA, 1996), p. 193.
- ¹²U. Hwang *et al.*, *Astrophys. J.* **476**, 560 (1997).
- ¹³A. C. Fabian, K. A. Arnaud, M. W. Bautz, and Y. Tawara, *Astrophys. J.* **436**, 63 (1994).
- ¹⁴G. V. Brown *et al.*, *Ser. A, Astrophys. J.* **502**, 1015–1026 (1998).
- ¹⁵P. Beiersdorfer *et al.*, *Phys. Rev. A* **46**, 3812 (1992).
- ¹⁶V. Decaux *et al.*, *Astrophys. J.* **443**, 464 (1995).
- ¹⁷P. Beiersdorfer *et al.*, *Rev. Sci. Instrum.* **68**, 1077 (1997).
- ¹⁸P. Beiersdorfer and B. Wargelin, *Rev. Sci. Instrum.* **65**, 13 (1994).
- ¹⁹A. Burek, *Space Sci. Instrum.* **2**, 53 (1976).
- ²⁰C. J. Borkowski and M. K. Kopp, *J. Appl. Crystallogr.* **11**, 430 (1978).
- ²¹www.cxro.lbl.gov
- ²²D. W. Savin, P. Beiersdorfer, J. C. López-Urrutia, V. Decaux, E. M. Gullikson, S. M. Kahn, D. A. Liedahl, K. J. Reed, and K. Widmann, *Astrophys. J.* **470**, 73 (1996).
- ²³J. H. Parkinson, *Astron. Astrophys.* **24**, 215 (1973).
- ²⁴J. R. Oppenheimer, *Z. Phys.* **43**, 27 (1927).
- ²⁵I. Percival and M. Seaton, *Philos. Trans. R. Soc. London Ser. A* **251**, 113 (1958).
- ²⁶P. Beiersdorfer *et al.*, *Rev. Sci. Instrum.* **68**, 1073 (1997).
- ²⁷B. L. Henke, E. M. Gullikson, and J. C. Davis, *At. Data Nucl. Data Tables* **54**, 181 (1993).